Available online at www.sciencedirect.com
SCIENCE DIRECT®
Optics Communications 244 (2005) 355–365
OPTICS COMMUNICATIONS
www.elsevier.com/locate/optcom

Spatiotemporal emission dynamics of a broad-area semiconductor laser in an external cavity: stabilization and feedback-induced instabilities

Shyam K. Mandre *, Ingo Fischer, Wolfgang Elsäßer

Institute of Applied Physics, Darmstadt University of Technology, Schlossgartenstrasse 7, D-64289 Darmstadt, Germany

Received 13 July 2004; received in revised form 20 September 2004; accepted 23 September 2004

Abstract

We present investigations of the influence of spatially filtered optical feedback on a broad-area semiconductor laser's spatiotemporal emission dynamics. Our measurements reveal the ambiguous effect of optical feedback on the emission behavior of the broad-area laser. The measurements confirm that optical feedback can have a stabilizing effect on the inherent spatiotemporal instabilities exhibited by solitary broad-area lasers. Moreover, at high feedback strengths, we observe feedback-induced instabilities instead of the inherent spatiotemporal instabilities, thus, a destabilizing effect of optical feedback. The results are complemented and extended by measurements of the optical spectrum, which demonstrate that stabilization of the emission dynamics by optical feedback is accompanied by a drastic reduction of the number of modes contributing to the emission.

PACS: 42.55.Px; 42.65.Sf; 42.60.Da; 05.45.Gg
Keywords: Broad-area semiconductor laser; Spatiotemporal dynamics; Delay-instabilities; Chaos control; Laser resonators

1. Introduction and overview

Broad-area semiconductor lasers (BALs) are promising devices for compact and efficient high-power applications. The high output powers in BALs are achieved by enlargement of the emitting width from a few μm in narrow-stripe edge-emitting semiconductor lasers (SLs) to typically 50–200 μm in BALs. With these widths, output powers of several Watts from a single device are possible [1]. However, due to the enlarged emitting widths of BALs, their emission is governed by complex, spatiotemporal emission dynamics [2–5]

* Corresponding author. Tel.: +49 (0) 6151 164086; fax: +49 (0) 6151 163022.
E-mail address: shyam.mandre@physik.tu-darmstadt.de (S.K. Mandre).

0030-4018/$ - see front matter © 2004 Elsevier B.V. All rights reserved.
doi:10.1016/j.optcom.2004.09.058

along with static beam filamentation [6,7], resulting from the nonlinear interaction between the optical field and the semiconductor medium [8]. Associated herewith, BALs exhibit an optical spectrum containing a multiplicity of longitudinal and lateral modes, and a wide double-lobed far-field intensity distribution. Altogether, these emission properties prevent wider application of BALs in many conceivable fields, i.e., spectroscopy, material processing, or medicine.

Various schemes have been proposed to improve the beam quality of BALs. They include concepts such as contact profiling [9,10], injection locking [11,12], and facet etching [13,14] and have indeed been successful in improving the static and spectral emission characteristics of BALs. Further promising concepts consist of optical feedback schemes, which allow compact solutions without the need of additional lasers or specifically designed BAL-structures. These concepts include feedback schemes employing gratings [15,16] or etalons [17] as spectral filters, spatial filters [18–22], a combination of both [23], or even phase conjugate feedback [24–26]. While the experiments implementing these various concepts concentrate on the *static* emission properties, our work concentrates on the *stabilization of* the spatiotemporal *emission dynamics* of BALs in optical feedback configurations, the capability of which has been demonstrated numerically [18–20,27]. Indeed, we have shown that our concept of spatially filtered optical feedback is capable of stabilizing a BAL's spatiotemporal emission dynamics [28]. However, in order to understand the concept of stabilization via optical feedback, more detailed investigations and characterization of the effects of feedback on the emission of BALs are necessary. A better understanding will also help to optimize the stabilization.

Studying the effects of optical feedback on BALs, one has to keep in mind that optical feedback can as well have the contrary effect of inducing instabilities in the emission of SLs. This well-known effect has been extensively studied for narrow-stripe SLs, where different regimes have been identified: an important distinction between long and short cavities has been made recently [29,30]. In the long cavity regime, where the internal relaxation oscillation frequency is larger than the external cavity frequency, the effects range from stable emission to external cavity-induced instabilities such as low frequency fluctuations and coherence collapse (see e.g. [31]). When the external cavity frequency is in the order of, or even exceeds the relaxation oscillation frequency – referred to as the short cavity regime – an additional dynamical regime consisting of regular and irregular pulse packages has been identified, thus contributing to the vast spectrum of dynamical regimes which have been found in narrow-stripe SLs in external cavities. However, based on the fact that BALs, unlike narrow-stripe SLs, exhibit spatiotemporal emission dynamics in the solitary case (i.e., without feedback), we cannot readily conclude that optical feedback has a similar effect on the emission of BALs as it has on narrow-stripe SLs. Therefore, taking into account the stabilizing, as well as destabilizing effect that optical feedback is known to have on the emission properties of narrow-stripe SLs, detailed studies of the influence of optical feedback on the emission properties of BALs are indispensable.

In this paper we present investigations of a BAL in a short, spatially filtering external cavity. In particular, we discuss the dependency of the BAL's emission properties on the optical feedback strength. Our results show that the feedback strength has a profound influence on the character of the emission dynamics ranging from feedback-induced instabilities to control of the internal (solitary laser's) spatiotemporal emission dynamics. Furthermore, we discuss the effect of the optical feedback on the optical spectrum of the BAL, comparing the solitary BAL's emission with the emission under feedback. The measurements show that the spectral properties are connected to the dynamical behavior of the BAL's emission.

This paper is structured as follows. Section 2 describes the experimental setup. In Section 3, we present the results of our investigations on the emission dynamics of a BAL without and with feedback. We demonstrate the influence of the feedback strength on the emission behavior for various feedback strengths. In Section 4, the effect of optical feedback on the optical spectrum of a

BAL is presented and discussed. Finally, in Section 5, our conclusions are presented.

2. Experimental setup

Fig. 1 depicts a schematic of the experimental setup, showing the plane along the slow axis [32]. The commercial, index-guided BAL with a stripe width of 100 μm emits a nominal output power of 1000 mW at 807 nm. Its solitary threshold current is I_{thr} = 302 mA. To realize a spatially filtering feedback configuration, a semitransparent mirror is used in combination with an aspheric lens. The lens collimates the beam in the direction of the fast axis [33]. Thereby, due to astigmatism of the emitted beam, the slow axis is initially focused and is subsequently divergent. By placing the mirror at a distance L from the laser facet, beyond the focusing point of the beam, we have the effect of a spatial filter since only paraxial parts of the beam are reflected back into the laser. The feedback phase, i.e., the optical phase accumulated within the external cavity, can be controlled by varying the external cavity length on the optical wavelength scale using a piezo transducer (PZT). The feedback strength is varied with neutral density filters (NDFs) placed within the cavity. The power spectrum of the intensity is measured by detecting the light with an avalanche photo diode (APD) with a 3-dB-cut-off frequency of approximately 2.5 GHz in combination with an electrical spectrum analyzer (ESA, Tektronix 2755AP). For this, an image of the lateral spatial dimension of the laser facet is projected onto the APD. Since the detector's area is significantly smaller than the width of the image, we can select different lateral positions of the facet by moving the detector across the image, thereby allowing a moderate spatial resolution estimated to be in the order of one tenth of the laser facet's width. The feedback strength is related to the threshold current reduction $\Delta I_{thr,FB}/I_{thr}$ ($\Delta I_{thr,FB} = I_{thr} - I_{thr,FB}$ and $I_{thr,FB}$ is the threshold current of the BAL subject to feedback), which is determined via a P–I curve measured with a Si-PIN diode. Additionally, we can monitor the spatially resolved optical spectrum of the BAL using a Czerny–Turner Imaging Spectrometer and a CCD camera, which enables us to examine the effect of the feedback on the optical spectrum and the modal spatial profiles simultaneously.

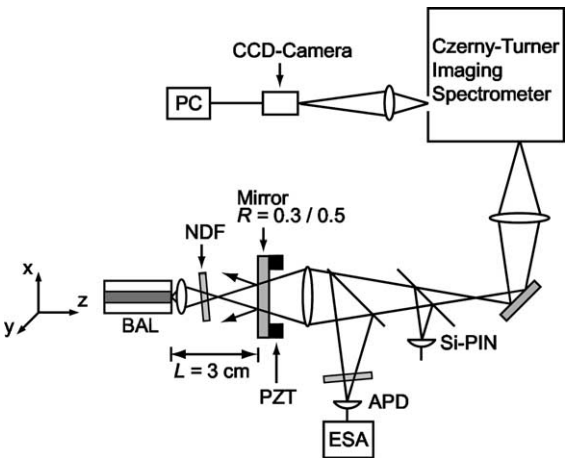

Fig. 1. Schematic of the experimental setup. The lateral (slow axis [32]) dimension of the BAL lies in the direction of the x-axis.

3. Broad-area laser dynamics

3.1. Solitary laser

Before discussing the effects of feedback on the emission dynamics of the BAL, power spectra of the solitary BAL, i.e. the laser without feedback, are depicted in Fig. 2. For this, the mirror was removed from the setup described above. These power spectra were obtained at a fixed, nearly central lateral position of the facet's image on the APD. While the power spectra at various positions show quantitative variation, we have observed qualitative agreement among different facet positions. The power spectra show that the BAL exhibits dynamics, whose complexity increases with pump current. At a low pump current of I_{pump} = 330 mA (Fig. 2(a)) only few, dominant peaks appear. The positions of these peaks shift slightly with variation of the pump current. Furthermore, at I_{pump} = 420 mA in Fig. 2(b), the number of peaks and their widths increase, leading to a broad peak at approximately 2 GHz along

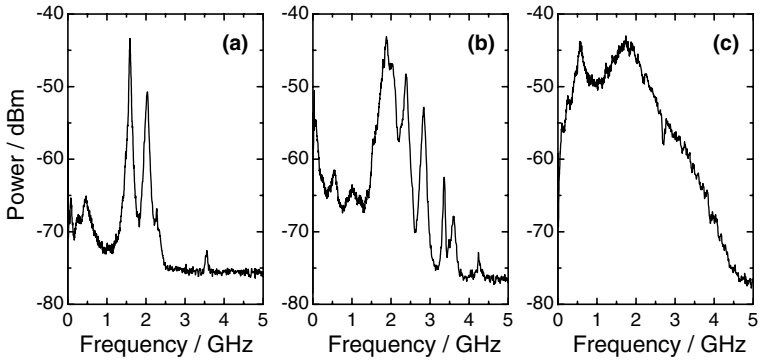

Fig. 2. Power spectra of the solitary BAL, (a) at I_{pump} = 330 mA, (b) 420 mA, and (c) 900 mA.

with other peaks at higher frequencies. Finally, in Fig. 2(c), at a pump current of I_{pump} = 900 mA, we find a broad spectrum limited only by the detector's bandwidth. We note that the signal for I_{pump} = 900 mA is much stronger as compared to the previous two measurements, therefore, it has been attenuated by 10 dB for this measurement. The broad spectrum indicates broadband chaotic emission dynamics of the solitary BAL, which cannot be the result of beating of various lateral modes. The spectra suggest that with increasing pump current, the interplay of nonlinear and local mechanisms increasingly determines the emission characteristics. This interplay can be briefly described as follows [4,5,28]: spatial hole-burning leads to self-focusing, the effect of which is known as beam-filamentation. Diffraction couples light into the filaments' neighboring regions, where the optical gain is higher than in the regions of the filaments, thus contributing to the spatiotemporal instabilities. Carrier diffusion opposes this process as it tends to fill up the holes. The interplay of these mechanisms leads to the observed spatiotemporal emission dynamics and, at high pump currents, even to chaotic emission. Therefore, unlike standard edge-emitting SLs, BALs already show complex emission dynamics in the case of solitary operation, as is evident here, and has been discussed previously.

3.2. Influence of the feedback strength

To study the effect of feedback on the emission dynamics, we inserted a semitransparent mirror at a distance $L \sim 3$ cm from the laser facet along with variable NDFs as shown in Fig. 1. Here, the external cavity frequency amounting to 5 GHz exceeds the relaxation oscillation frequency of approximately 0.5–3 GHz (depending on the pump current). Therefore, we can classify this as a short-cavity-setup. The feedback strength was then controlled by the transmission of the NDFs and quantified by the threshold current reduction $\Delta I_{thr,FB}/I_{thr}$. Measured values for $\Delta I_{thr,FB}/I_{thr}$ range from 27% for the highest feedback strength to less than 1%. Intermediate values are 18%, 16%, 12%, 9%, 6%, and 2%. Correspondingly, the effective reflectivity of the external mirror ranges from 50% to approximately 1%. In the following paragraphs, we will discuss the emission behavior of the BAL for different feedback strengths, pump currents and feedback phases, which give rise to different dynamical regimes. Our measurements show that, depending on these parameters, the BAL's emission exhibits spatiotemporal instabilities, stabilized emission, or instabilities induced by delayed feedback from the short external cavity. Based on our measurements, we are then able to illustrate the influence of the feedback strength and pump current on the emission behavior in a parameter-space diagram.

Fig. 3 shows the emission behavior of the BAL at $\Delta I_{thr,FB}/I_{thr}$ = 2%. For this, we used NDFs with a one-way transmission of approximately 25% and a mirror with reflectivity of 30% giving rise to an effective external reflectivity of approximately 2%. The spectra of the BAL subject to feedback were obtained at approximately the same fixed lat-

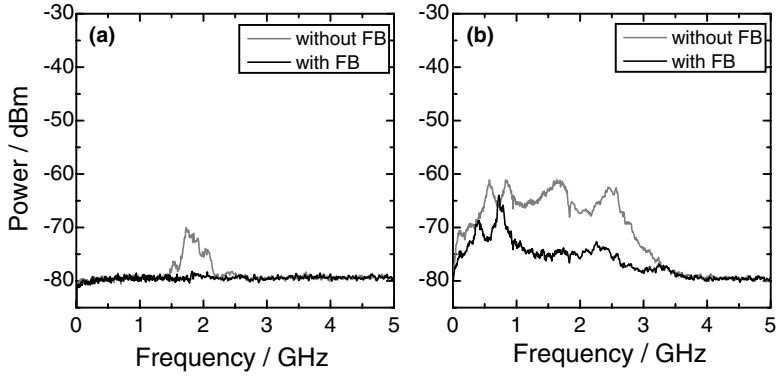

Fig. 3. Power spectra of the BAL subject to feedback (FB) with $\Delta I_{thr,FB}/I_{thr} = 2\%$ (black) and the solitary BAL (gray) at: (a) $I_{pump} = 400$ mA, and (b) 750 mA. In both spectra, the differences in output powers between the BAL subject to feedback and the solitary BAL are less than 5%.

eral position of the facet's image on the APD as the power spectra of the solitary BAL. Nevertheless, the characteristic emission properties at different feedback strengths discussed in the following paragraphs could also be verified qualitatively for other positions. The measurements with $\Delta I_{thr,FB}/I_{thr} = 2\%$ show that we can stabilize the BAL's emission for a wide pump-current-range. Fig. 3(a) depicts a flat power spectrum of the BAL subject to feedback (black) and a power spectrum indicating spatiotemporal instabilities of the solitary BAL (gray), both at $I_{pump} = 400$ mA. Due to the small feedback strength, the difference in output power between the two cases is less than 5%. For this direct comparison, the case without feedback was measured by tilting the mirror around the x-axis (cf. Fig. 1) until the BAL was no longer subject to feedback. As the other parameters (NDFs within the cavity and mirror reflectivity) remain unchanged, a direct comparison of the power spectra with and without feedback is possible. Such flat power spectra of the BAL's emission when subject to feedback were obtained from low pump currents up to $I_{pump} \sim 650$ mA. At these high pump currents, the feedback phase gains importance. Depending on the feedback phase, the power spectrum shows internal spatiotemporal instabilities, or stabilized emission. Similar influence of the feedback phase on stabilization has been observed in numerical analysis [27,34]. There, the feedback phase determines whether specific lateral modes experience constructive or destructive interference, thus leading to stabilized emission or the predominance of internal spatiotemporal instabilities. However, since the models describe single-longitudinal-mode operation, a more detailed comparison with the behavior observed here may not be appropriate, as the BAL used for these measurements exhibits multi-longitudinal-mode emission. Furthermore, in contrast to the references, we have employed a spatially filtering feedback configuration, which is designed to prefer the fundamental mode. Nevertheless, we assume that the mechanism described in [27,34] may also be relevant for the behavior observed here. At $I_{pump} = 750$ mA no complete suppression, however, partial suppression can still be observed. This is shown in Fig. 3(b), where power spectra of the BAL's emission with (black) and without feedback (gray) are depicted for $I_{pump} = 750$. Again, the difference in output power is less than 5%. In fact, partial suppression of the spatiotemporal instabilities prevailed even up to a pump current of $I_{pump} = 850$ mA. We could determine a suppression factor of the spatiotemporal instabilities in this configuration of typically 10–15 dB up to $I_{pump} = 850$ mA. These measurements confirm previous investigations [28] by demonstrating that spatially filtered optical feedback is capable of stabilizing the emission dynamics of BALs. As discussed in the introduction, optical feedback can also have a destabilizing effect on the emission

of narrow-stripe SLs. To investigate whether similar effects occur in the emission of BALs, we have studied the influence of the feedback strength on the emission behavior of a BAL. Indeed, the measurements show that the emission behavior is strongly dependent on the feedback strength and that optical feedback can have destabilizing effects on BALs under certain circumstances.

Stabilization of the BAL's spatiotemporal instabilities was achieved at $\Delta I_{thr,FB}/I_{thr} = 2\%$, which corresponds to comparatively weak feedback. As Fig. 4 shows, the emission behavior of the BAL completely changes when subject to comparatively strong feedback at $\Delta I_{thr,FB}/I_{thr} = 27\%$. For this, we used a mirror with reflectivity of 50%. At low pump currents, the internal emission dynamics of the solitary BAL (cf. Fig. 2(a)) is suppressed, as can be seen in Fig. 4(a). Instead, the laser now exhibits pulsations with approximately 0.4 GHz repetition rate. These so-called pulse packages (PP) have been identified as a typical phenomenon induced solely by the short external cavity. The existence of these PPs has been investigated numerically and experimentally for narrow-stripe SLs in the short cavity regime. In particular, strong pump-current-dependency and feedback-phase-dependency of the PPs have been shown [29,30], which we could also observe in our measurements. With increasing pump current, the peak-widths in the power spectrum increase corresponding to increasing irregularity of the PPs. Finally, at moderate to high pump currents, the PPs end up in highly complex emission dynamics, i.e., the dynamical regime of coherence collapse. As an example, the power spectrum at $I_{pump} = 400$ mA is shown in Fig. 4(b), in which the PPs can still be identified. Thus, the power spectra reveal that the internal instabilities of the BAL are replaced by feedback-induced instabilities.

The phase dependency of the PPs is demonstrated in Fig. 5. For these measurements, we used appropriate NDFs and the 30%-mirror, which resulted in $\Delta I_{thr,FB}/I_{thr} = 16\%$. As is shown here, the feedback phase plays a vital role in the occurrence of the PPs. The power spectra in Figs. 5(a) and (b) both display the emission dynamics at a pump current of $I_{pump} = 300$ mA. By varying the feedback phase, we could switch between regular PPs and a broader power spectrum indicating complex dynamics. Again, at higher pump currents, complex temporal dynamics, i.e., coherence collapse was observed.

It is now evident that optical feedback can have a stabilizing or destabilizing, thus, an ambivalent effect on the emission behavior of BALs. To illustrate this ambivalent effect, we have summarized the observed emission behavior for various feedback strengths corresponding to different threshold current reductions in a parameter-space diagram depicted in Fig. 6. In analogy to similar plots for narrow-stripe SLs [35,36], the vertical and horizontal axes correspond to the pump current I_{pump} and the threshold current reduction $\Delta I_{thr,FB}/I_{thr}$, respectively. The threshold currents $I_{thr,FB}$ under feedback resulting from the intracavity NDFs and mirror reflectivity are indicated by

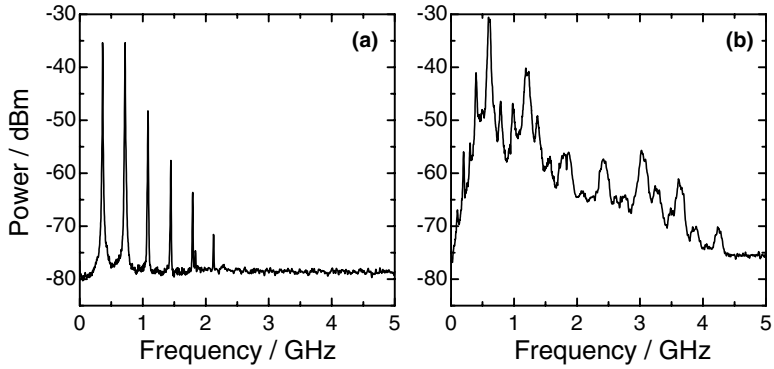

Fig. 4. Power spectra of the BAL under feedback with $\Delta I_{thr,FB}/I_{thr} = 27\%$. (a) $I_{pump} = 290$ mA, and (b) 400 mA.

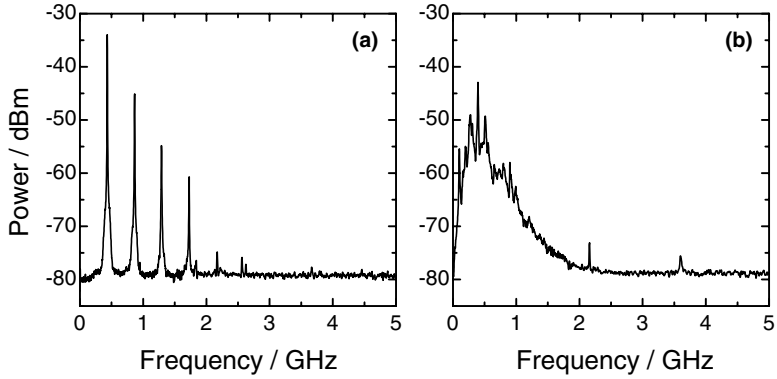

Fig. 5. Power spectra of the BAL under feedback with $\Delta I_{thr,FB}/I_{thr} = 16\%$. (a) and (b) $I_{pump} = 300$ mA, but with different relative feedback phases.

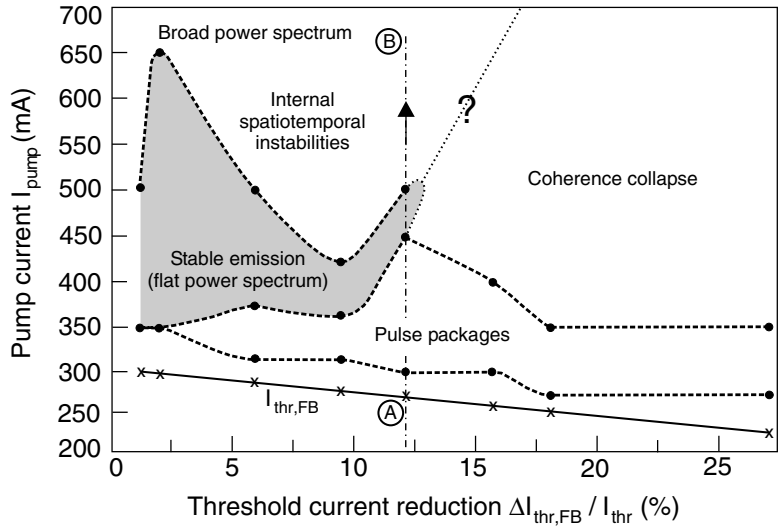

Fig. 6. The dynamical behavior of the BAL subject to feedback in an I_{pump} vs. $\Delta I_{thr,FB}/I_{thr}$-parameter-space diagram. The dots correspond to approximate transition points between dynamical regimes as obtained by the measurements. The dashed lines connecting the dots are a guide to the eye to roughly distinguish between the different regimes.

crosses. The dots are placed at transition points between two dynamical regimes obtained by the recorded power spectra. They also indicate the threshold current reductions at which the measurements were performed. The dashed lines connecting the dots are a guide to the eye to distinguish the different dynamical regimes. The lowest dashed line, which proceeds along the solid line representing $I_{thr,FB}$, marks the limit below which the intensity on the APD is not sufficient for a characterization. Therefore, we cannot assign the area below this dashed line to any dynamical regime. By increasing the pump current (moving upward in the plot) from any given threshold current, one passes through different dynamical regimes. As an example, we describe the development of the emission behavior for $\Delta I_{thr,FB}/I_{thr} = 12\%$ by starting from $I_{thr,FB} = 265$ mA denoted as point "A" and then moving upward (increasing pump current) along the vertical dash-dotted line, which ends at point "B". By increasing the pump current from the starting point, one initially passes

through the dynamical regime of PPs. When the pump current is increased further, the BAL exhibits a stable-emission-window, where the internal spatiotemporal instabilities are completely suppressed, and the externally induced PPs do not occur. For $\Delta I_{thr,FB}/I_{thr} = 12\%$ this stable-emission-window lies at pump currents between $I_{pump} = 450$ mA and $I_{pump} = 500$ mA. As an example, Fig. 7(a) depicts an almost flat power spectrum measured at $I_{pump} = 450$ mA. At higher pump currents (further up along the vertical dash-dotted line in Fig. 6) the power spectra show onset of dynamics, as in Fig. 7(b) at $I_{pump} = 700$ mA. Here, the power spectrum resembles those of the solitary BAL suggesting that the dynamics is now dominated by the internal spatiotemporal instabilities. Finally, at even higher pump currents (denoted as point "B" in Fig. 6), we obtain broad power spectra.

At feedback strengths corresponding to $\Delta I_{thr,FB}/I_{thr} > 12\%$ (16%, 18%, and 27%), the plot shows the occurrence of PPs at low pump currents, while at higher pump currents, coherence collapse is observed. Here, the emission is governed by dynamics induced by the external cavity. For $\Delta I_{thr,FB}/I_{thr} \leqslant 12\%$, the current range in which feedback-induced instabilities occur shrinks. For low pump currents, the BAL's emission still exhibits PPs. However, for moderate pump currents, we now observe stable-emission-windows. By reducing the feedback strength, the pump current-range of the stable-emission-window is extended up to the optimal condition at $\Delta I_{thr,FB}/I_{thr} = 2\%$, which corresponds to an effective external reflectivity of 2%. Here, suppression is most significant over the widest pump-current-range among the feedback strengths investigated. For even higher pump currents, the BAL's emission exhibits suppressed internal spatiotemporal instabilities. At the lowest investigated feedback strength of $\Delta I_{thr,FB}/I_{thr} = 1\%$, the range of stabilization again shrinks compared to the optimal condition. This is in accordance with the fact, that the solitary BAL exhibits spatiotemporal dynamics over the entire pump-current-range.

The question mark and the dotted line in the diagram indicate a transition region of internal instabilities, stabilized emission, and feedback-induced instabilities around $\Delta I_{thr,FB}/I_{thr} = 12\%$. In this region, in addition to the pump current and feedback strength, the feedback phase has an effect on the emission dynamics. For example, at $\Delta I_{thr,FB}/I_{thr} = 9\%$, we could also observe feedback-induced instabilities at pump currents above the stable emission regime, even though the emission was dominated by internal spatiotemporal instabilities. This interesting region, where four different dynamical regimes meet, deserves further detailed characterization.

This parameter-space diagram illustrates the ambivalent effect of optical feedback on the BAL's emission dynamics. While the internal spatiotemporal instabilities are suppressed (or even stabilized) for low feedback strengths, they are replaced by feedback-induced instabilities at high feedback strengths.

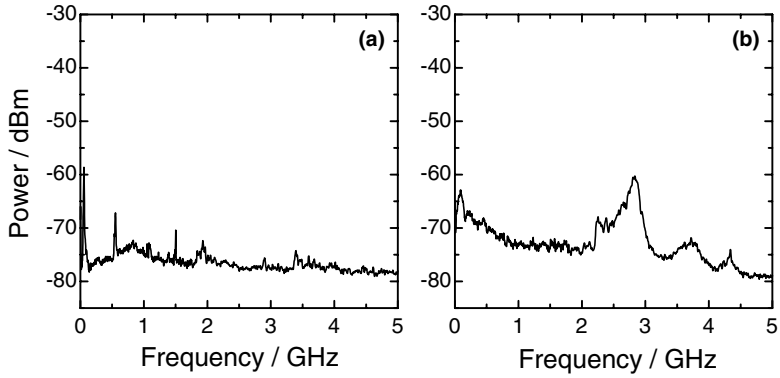

Fig. 7. Power spectra of the BAL under feedback with $\Delta I_{thr,FB}/I_{thr} = 12\%$. (a) $I_{pump} = 450$ mA and (b) 700 mA.

4. Optical spectrum

The power spectra reveal a manifold of dynamical emission characteristics of the solitary BAL and of the BAL subject to optical feedback. As has been stated before, the spatiotemporal emission dynamics of BALs is associated with multi-longitudinal and multilateral-mode emission. In order to get more insight into the link between the dynamical properties of the BAL with and without feedback and the optical spectrum, we have used an imaging spectrometer to measure spatially resolved optical spectra, which are depicted in Figs. 8 and 9, respectively. The horizontal axis depicts the wavelength and the vertical axis depicts the position on the laser facet. The images show approximately 0.7 nm long sections of the typically 1–2 nm wide optical spectra. Fig. 8(a) shows an optical spectrum of the solitary BAL at $I_{\text{pump}} = 420$ mA. Here, we can identify eight longitudinal modes. In addition, each longitudinal mode consists of a group of lateral modes, therefore, we can refer to the groups as longitudinal-mode families. Fig. 8(b) depicts an optical spectrum of the solitary BAL at $I_{\text{pump}} = 750$ mA. Here, the number of lateral modes contributing

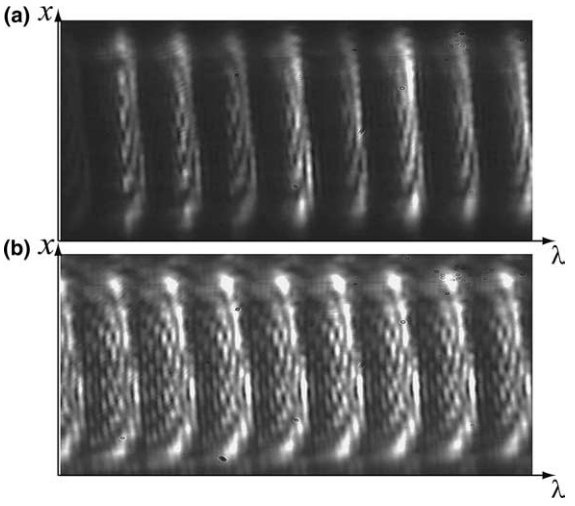

Fig. 8. Optical spectra of the solitary BAL at: (a) $I_{\text{pump}} = 420$ mA, and (b) at $I_{\text{pump}} = 750$ mA. The horizontal axis which depicts the wavelength shows a ~0.7 nm wide section of the typically 1–2 nm spectrum at ~807 nm. The vertical axis shows the position on the 100-μm broad laser facet.

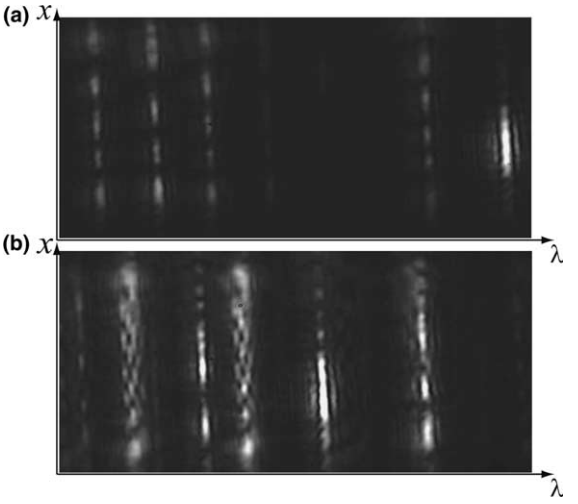

Fig. 9. Optical spectra of the BAL with $\Delta I_{\text{thr,FB}}/I_{\text{thr}} = 2\%$ at: (a) $I_{\text{pump}} = 400$ mA, and (b) at $I_{\text{pump}} = 750$ mA. The horizontal axis which depicts the wavelength shows a ~0.7 nm wide section of the typically 1–2 nm spectrum at ~807 nm. The vertical axis shows the position on the 100-μm broad laser facet.

to the emission has increased significantly. Thus, as these two optical spectra show, the number of longitudinal and, especially, higher order lateral modes increases with increasing pump current.

To demonstrate the influence of optical feedback on the optical spectra, Fig. 9 shows optical spectra of the BAL subject to feedback with $\Delta I_{\text{thr,FB}}/I_{\text{thr}} = 2\%$ at: (a) $I_{\text{pump}} = 400$ mA, and (b) $I_{\text{pump}} = 750$ mA. These two optical spectra correspond to the rf-spectra of the stabilized BAL discussed in Section 3.2 (Figs. 3(a) and (b), respectively). The optical spectra reveal a dramatic reduction of the number of modes contributing to the emission as compared to the solitary BAL's spectra (cf. Figs. 8(a) and (b), respectively). In Fig. 9(a), the intensity of the fundamental lateral mode is about 2.5 times larger than that of the higher order modes, whereas in the solitary BAL's spectrum, the intensities of the lateral modes within a longitudinal-mode family are rather evenly distributed. This underlines that, due to the spatial filter, the fundamental mode is preferred [28], even though the BAL's spatial gain profile competes against preference of fundamental-mode operation, thereby weakly exciting higher order lateral modes. Apart from favoring fundamental-mode

emission, the spatially filtering feedback applied here stabilizes the BAL's emission, as was discussed in the case of Fig. 3(a). Furthermore, our measurements demonstrate a direct link between the BAL's spatiotemporal instabilities and its spectral emission properties. This link is revealed by the collapse of the broadband optical spectrum in the case of solitary operation to a spectrum consisting of only few modes when the emission is stabilized (cf. Figs. 9(a) and 3(a)). By increasing the pump current to $I_{\text{pump}} = 750$ mA the spatiotemporal instabilities arise again, but still experience partial suppression of approximately 10 dB (cf. Fig. 3(b)). Indeed, Fig. 9(b) shows that the reduction of modes prevails at this high pump current even though the number of modes in the optical spectrum has increased compared to Fig. 9(a). This increase in the number of modes at higher pump currents represents the spatiospectral consequences of the increasing spatiotemporal dynamics indicated by the rf-spectrum in Fig. 3(b). Due to the nonlinear and local mechanisms mentioned in Section 3.1, the spatiotemporal instabilities arise again. Regarding the optical spectrum, the emission is diverted away from the fundamental mode and increasingly consists of higher order lateral modes whose modal profiles better accommodate the gain defined by the pump profile. Finally, the reduction of modes when feedback is applied is particularly remarkable, as we have not employed any spectral filters in our configuration. The stabilizing effect of the spatially filtered optical feedback alone leads to reduction of the number of modes in the optical spectrum.

5. Conclusions

We have investigated the influence of optical feedback on the emission dynamics and on the optical spectrum of a BAL in a short-cavity-setup with the feedback strength as the control parameter. Our studies show a variety of dynamical regimes ranging from feedback-induced regular dynamics, complex or even chaotic dynamics, to suppression of the dynamics altogether, thus, underlining the ambivalent influence of optical feedback. The results demonstrate the occurrence of the various dynamical regimes and that they can be controlled via the feedback strength and the pump current. Furthermore, with respect to stabilization, we could identify an optimal feedback strength, at which suppression is achieved over the widest pump-current-range. This low feedback strength, related to the low threshold current reduction of 2%, indicates the possibility of using mirrors with low reflectivity, thereby allowing high outcoupling rates. In the configuration discussed here, we can estimate the effective reflectivity to approximately 2%. We therefore demonstrate that stable and high-power emission can be achieved with BALs.

Measurements of the optical spectrum have shown that the solitary BAL's numerous longitudinal and lateral modes collapse to a few modes when the BAL's spatiotemporal instabilities are suppressed by optical feedback. We could therefore show that the spectral properties are directly connected to the dynamical behavior of the BAL's emission.

For a comprehensive understanding of BALs in external cavities, further investigations of the effect of the feedback phase and of the external cavity length are essential. Nevertheless, the results presented here provide a substantial overview of the emission properties of a BAL with optical feedback from a short external cavity.

Acknowledgments

The authors thank the Federal Ministry for Research and Education (BMBF) and the Volkswagen Foundation for financial support.

References

[1] E. Gehrig, O. Hess, in: R. Diehl (Ed.), Topics in Applied Optics, vol. 3, Springer, Heidelberg, 2000, p. 55.
[2] H. Adachihara, O. Hess, E. Abraham, P. Ru, J.V. Moloney, J. Opt. Soc. Am. B 10 (1993) 658.
[3] O. Hess, S.W. Koch, J.V. Moloney, IEEE J. Quantum Electron. 31 (1995) 35.
[4] I. Fischer, O. Hess, W. Elsäßer, E. Göbel, Europhys. Lett. 35 (1996) 579.

[5] T. Burkhard, M.O. Ziegler, I. Fischer, W. Elsäßer, Chaos, Solitons Fract. 10 (1999) 845.
[6] G.H.B. Thompson, Opto-Electronics 4 (1972) 257.
[7] R.J. Lang, A.G. Larsson, J.G. Cody, IEEE J. Quantum Electron. 27 (1991) 312.
[8] J.R. Marciante, G.P. Agrawal, IEEE J. Quantum Electron. 32 (1996) 590.
[9] C. Lindsey, P. Derry, A. Yariv, Appl. Phys. Lett. 47 (1985) 560.
[10] P.M.W. Skovgaard, P. O'Brien, J.G. McInerney, Electron. Lett. 34 (1998) 1950.
[11] L. Goldberg, M.K. Chun, Appl. Phys. Lett. 53 (1988) 1900.
[12] G.L. Abbas, S. Yang, V.W.S. Chan, J.G. Fujimoto, IEEE J. Quantum Electron. 24 (1988) 609.
[13] Z. Bao, R.K. DeFreez, P.D. Carleson, C. Largent, C. Moeller, G.C. Dente, Electron. Lett. 29 (1993) 1597.
[14] S.A. Biellak, C.G. Fanning, Y. Sun, S.S. Wong, A.E. Siegman, IEEE J. Quantum Electron. 33 (1997) 219.
[15] H. Sato, H. Asakura, M. Fukai, N. Suzuki, IEEE J. Quantum Electron. QE-18 (1982) 155.
[16] M. Pan, D.J. Evans, G.R. Gray, L.M. Smith, R.E. Benner, C.W. Johnson, D.D. Knowlton, J. Opt. Soc. Am. B 15 (1998) 2531.
[17] W. Nagengast, K. Rith, Opt. Lett. 22 (1997) 1250.
[18] M.E. Bleich, D. Hochheiser, J.V. Moloney, J.E.S. Socolar, Phys. Rev. E 55 (1997) 2119.
[19] D. Hochheiser, J.V. Moloney, J. Lega, Phys. Rev. A 55 (1997) R4011.
[20] C. Simmendinger, D. Preißer, O. Hess, Opt. Express 5 (1999) 48.
[21] S. Wolff, H. Fouckhardt, Opt. Express 7 (2000) 222.
[22] S. Wolff, A. Rodionov, V.E. Sherstobitov, H. Fouckhardt, IEEE J. Quantum Electron. 39 (2003) 448.
[23] V. Raab, D. Skoczowsky, R. Menzel, Opt. Lett. 27 (2002) 1995.
[24] T. Omatsu, A. Katoh, K. Okada, S. Hatano, A. Hasegawa, M. Tateda, I. Ogura, Opt. Commun. 146 (1998) 167.
[25] S. Hatano, T. Omatsu, A. Hasegawa, M. Tateda, I. Ogura, Jpn. J. Appl. Phys. 38 (1999) 3522.
[26] J.S. Lawrence, D.M. Kane, J. Lightwave Technol. 20 (2002) 100.
[27] J. Martin-Regalado, G.H.M. Tartwijk, S. Balle, M. San Miguel, Phys. Rev. A 54 (1996) 5386.
[28] S.K. Mandre, I. Fischer, W. Elsäßer, Opt. Lett. 28 (2003) 1135.
[29] T. Heil, I. Fischer, W. Elsäßer, A. Gavrielides, Phys. Rev. Lett. 24 (2001) 243901.
[30] T. Heil, I. Fischer, W. Elsäßer, B. Krauskopf, K. Green, A. Gavrielides, Phys. Rev. E 67 (2003) 066214.
[31] I. Fischer, T. Heil, W. Elsäßer, in: Bernd Krauskopf, Daan Lenstra (Eds.), Nonlinear Laser Dynamics: Concepts, Mathematics, Physics, and Applications International Spring School, AIP Conf. Proc. No. 548, AIP, Melville, NY, 2000, p. 66.
[32] The slow axis is oriented in the lateral direction (x-axis, cf. Fig. 1) of the BAL where the beam divergence typically amounts to 5–10°.
[33] The fast axis' beam divergence is typically 25° and in the direction of the y-axis.
[34] M. Münkel, F. Kaiser, O. Hess, Phys. Rev. E 56 (1997) 3868.
[35] T. Heil, I. Fischer, W. Elsäßer, Phys. Rev. A 58 (1998) R2672.
[36] T. Heil, I. Fischer, W. Elsäßer, Phys. Rev. A 60 (1999) 634.